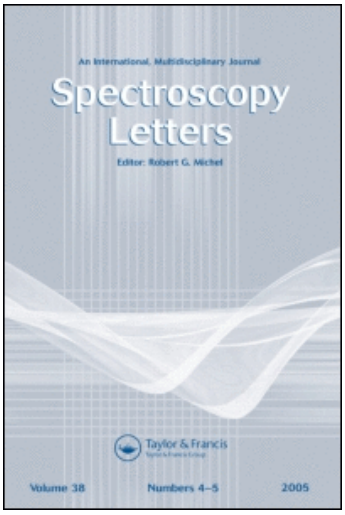

Spectroscopy Letters
Publication details, including instructions for authors and subscription information:
http://www.informaworld.com/smpp/title~content=t713597299

Influence of Solution Acidity on Structure of Actinocin Derivatives and Their Affinity to DNA Studied as a Function of pH by Raman Spectroscopy

Ju. N. Bliznyuk[a]; E. B. Kruglova[a]; T. V. Bolbukh[a]; D. V. Ovchinnikov[b]
[a] Institute of Radiophysics and Electronics of NAS of Ukraine, Kharkov, Ukraine [b] Department of Chemistry, St. Petersburg State Technological Institute, St. Petersburg, Russia

Online publication date: 01 December 2009

To cite this Article Bliznyuk, Ju. N. , Kruglova, E. B. , Bolbukh, T. V. and Ovchinnikov, D. V.(2009) 'Influence of Solution Acidity on Structure of Actinocin Derivatives and Their Affinity to DNA Studied as a Function of pH by Raman Spectroscopy', Spectroscopy Letters, 42: 8, 498 — 505
To link to this Article: DOI: 10.1080/00387010903022285
URL: http://dx.doi.org/10.1080/00387010903022285

Spectroscopy Letters, 42:498–505, 2009

ISSN: 0038-7010 print/1532-2289 online
DOI: 10.1080/00387010903022285

Taylor & Francis
Taylor & Francis Group

Influence of Solution Acidity on Structure of Actinocin Derivatives and Their Affinity to DNA Studied as a Function of pH by Raman Spectroscopy

Ju. N. Bliznyuk[1], E. B. Kruglova[1], T. V. Bolbukh[1], and D. V. Ovchinnikov[2]

[1]Institute of Radiophysics and Electronics of NAS of Ukraine, Kharkov, Ukraine
[2]Department of Chemistry, St. Petersburg State Technological Institute, St. Petersburg, Russia

ABSTRACT An important problem of molecular biophysics is the influence of pH and ionic strength of a solution on chemical structures and charge of biologically active substances. By means of pH titration and Raman spectroscopy methods, the influence of solution acidity on structural changes of actinocin derivatives was investigated, analogues to antitumor antibiotic actinomycin D. It has been shown that these ligands have different values of cation charges in neutral solutions. From analysis of Raman spectra, it was concluded that protonation of nitrogen atom and amino group of the phenoxazone ring starts only at $pH < 3.5$. It was shown that protonation of actinocin derivative with two amide groups (diaminoactinocin) occurred in two steps. Corresponding protonation constants for diaminoactinocin ($\log\ k_1 = 6.9 \pm 0.5$ and $\log\ k_2 = 5.3 \pm 0.1$) and for partially protonated actinocin derivative with three methylene groups in the side chains ($\log\ k = 5.3 \pm 0.1$) were obtained. Characteristic frequencies of Raman spectra for the basic functional C=O, C2$-NH_2$, C$-$C=C, and $-$N=C groups of phenoxazone chromophore of actinocin derivatives in protonated and nonprotonated states were determined. The different affinities of binding of variously charged ligands to DNA have also been demonstrated.

KEYWORDS actinocin derivatives, ionic strength, pH-metry, phenoxazone chromophore, Raman spectroscopy, thymus DNA

INTRODUCTION

Recently, it has been shown that derivatives of actinocin analogues to well-known antitumor antibiotic actinomycin D bind to DNA by intercalation of a chromophore ring of ligands into the base pairs of polynucleotide.[1] At the same time, the actinocin derivatives have shown the dependence of biological activity from the length of dimethylaminoalkyl side chains.[1,2] In this research, the influence of acidity (pH of solutions) on the structure of some actinocin derivatives was investigated: aminophenoxazone (Aph) (Fig. 1a)

Received 18 May 2007;
accepted 5 September 2008.

Address correspondence to Ju. N. Bliznyuk, Institute of Radiophysics and Electronics of NAS of Ukraine, Acad. Proskura str. 12, Kharkov, 61085, Ukraine. E-mail: bolbukh@ire.kharkov.ua

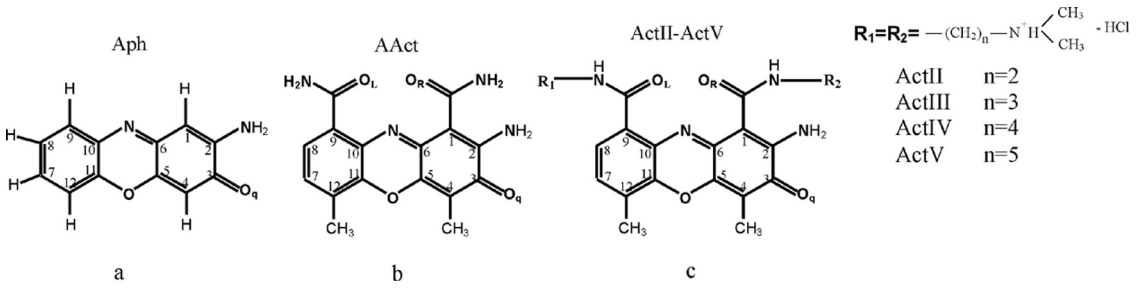

FIGURE 1 **Chemical structures of actinocin derivatives: aminophenoxazone (a), diaminoactinocin (b), and dimethylaminoalkyl derivatives ActII-ActV (c).**

and diaminoactinocin (AAct) (Fig. 1b) by the pH-titration and Raman spectroscopy. The pH-titration of actinocin derivatives having a different number of methylene groups in dimethylaminoalkyl side chains ActII–ActV (Fig. 1c) was also carried out. It was interesting to examine the influence of an ionic environment on the interaction of these ligands with DNA, as structures of both polynucleotide and drug molecules depend on composition of solvent, acidity (pH) of solutions, etc.[3–7]

EXPERIMENTAL SECTION

Titration of actinocin derivatives was carried out by the HCl solution with a constant concentration (pH 2.20). The pH of solutions was measured by an I-115 ionomer (Antex, LTD, Russia) with an accuracy of ± 0.05. Total concentrations of actinocin derivatives were determined by spectrophotometric measurements on the Specord M40 spectrophotometer (Carl Zeiss Jena, Germany). All samples of actinocin derivatives have been synthesized[8] and were used without additional purification. ActII–ActV concentrations were obtained by using molar extinction coefficient $\varepsilon_{400} = 1.6 \times 10^4\,\mathrm{M^{-1}cm^{-1}}$ at $\lambda = 400\,\mathrm{nm}$ corresponding to isobestic point of monomer-dimer equilibrium of ligands.[9] Molar extinction coefficients for Aph and AAct were determined by weighing $\varepsilon_{400} = 1.68 \cdot 10^3\,\mathrm{M^{-1}\,cm^{-1}}$ and $\varepsilon_{235} = 2.79 \cdot 10^3\,\mathrm{M^{-1}\,cm^{-1}}$. The pH titration curves of ligand water solutions were compared to the control pH titration curves of the HCl solution at the same HCl concentration. Triply distilled water was used to prepare solutions. The concentration of protons bound to ligands (ΔH^+) was determined by the difference between the control (without ligands) and experimental (in the presence of ligands) pH-dependences at the same total HCl concentration. ΔH^+_{max} is the maximum amount of ΔH^+ per mol of ligand. The distinction between two ActIII samples (marked as ActIII(1) and ActIII(2)) was also investigated, which showed the different affinities to DNA. Commercial calf thymus DNA from "Serva" (Germany) was used in this work. The concentration of DNA was determined by molar extinction coefficient $\varepsilon_{260} = 6.4 \times 10^3\,\mathrm{M^{-1}\,cm^{-1}}$. Corresponding Raman spectra in a spectral range 1200–1700 $\mathrm{cm^{-1}}$ were recorded on the Z-16 spectrometer (DILOR, France) with a double-monochromator. Our measurements were performed using 488-nm line of an Ar^+ ion laser (Innova, England). This line is close to the 440-nm absorption maximum of actinocin derivatives[10] satisfying the resonance Raman conditions. The energy of laser did not exceed 50 mW to avoid saturation effects and decomposition of the samples. The sample integrity was assessed by comparison of its absorption spectra in the visible spectral (VIS) range before and after data collection. The resolution of spectra was within $\pm 2\,\mathrm{cm^{-1}}$. All measurements were carried out at room temperature.

RESULTS AND DISCUSSION

Titration Curves and Raman Spectra of Aminophenoxazone

Figure 2a shows the titration curve of aminophenoxazone (Aph) in comparison with the control curve. It can be seen that the titration curve of aminophenoxazone at $9.4 \times 10^{-4}\,\mathrm{M}$ coincides, in general, with the control curve in $6.4 \div 3.5$ pH range (i.e., H^+ ions do not bind to Aph). At pH < 3.5, the actinocin derivatives can be hydrolyzed up to their initial reagent 4-methyl-3 hydroxyanthranyl acid[8] or are formed the 2-Deamino-2-hydroxyactinomycin D.[11,12] In this case, it is observed that the titration

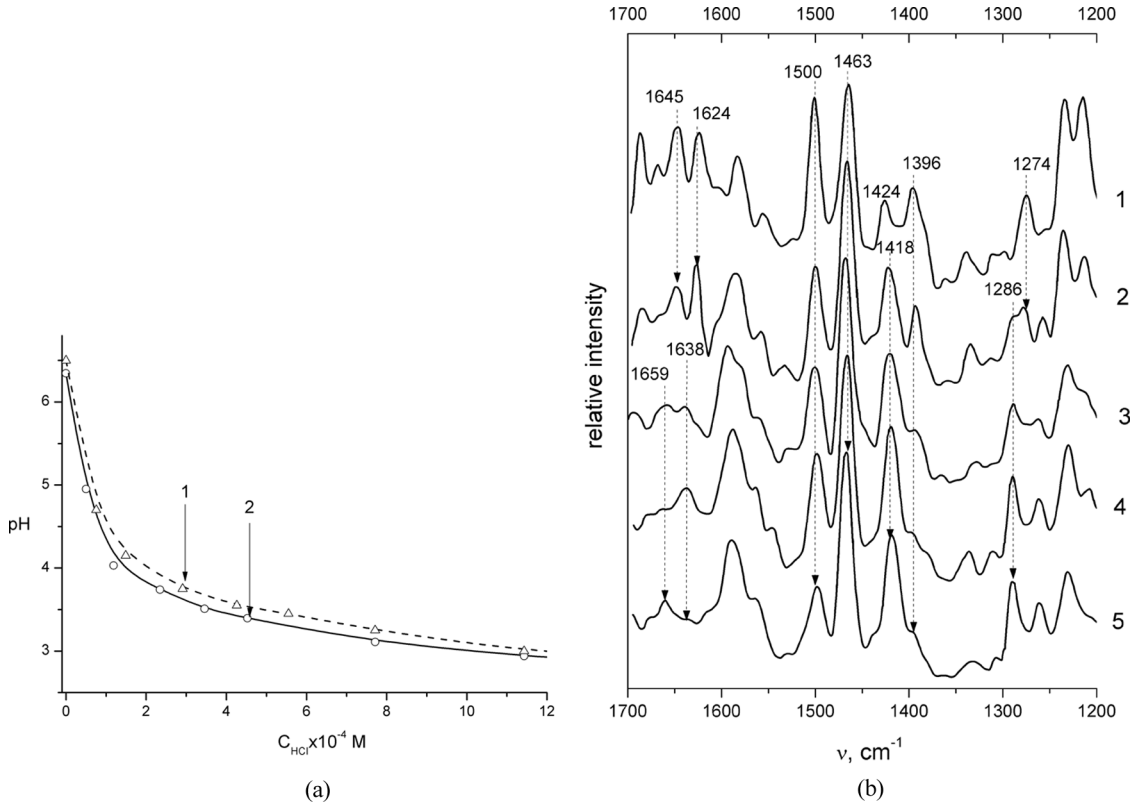

FIGURE 2 **(a) Experimental titration curves of (1) HCl solution (control) and (2) HCl solution in the presence of Aph. (b) Raman spectra of aminophenoxazone at pH (1) 6.40, (2) 3.35, (3) 3.00, (4) 2.95, and (5) 2.90. Concentration of Aph was constant $C_{Aph} = 9.4 \times 10^{-4}$ M. Error bars are smaller than the corresponding symbols at the titration curves.**

curve of aminophenoxazone lies a little lower than the control curve.

Raman spectra of aminophenoxazone at different pH-values are presented in Fig. 2b. Taking into account the Raman band assignments for actinomycin D,[13] the assignments of bands for Raman spectra of Aph have been made in a neutral solution; a band at 1274 cm^{-1} can be assigned to the symmetric stretching vibration of the endocyclic ν(φ−N=C) group; Raman bands in the range of ∼1390–1425 cm^{-1} correspond to vibration modes of the ν(C2−NH_2) amino group; $\nu \sim 1463$- and 1500-cm^{-1} bands can be assigned to asymmetric stretches of endocyclic ν(C−C=C) and ν(φ−N=C) groups of phenoxazone ring, respectively; the 1645 cm^{-1} band corresponds to the ν(C3=O_q) carbonyl group stretch.

It can be seen that the basic changes of spectral parameters for Aph start at pH < 3.5 (Fig. 2b), which agrees with the difference between the control and experimental curves in this range of pH. These changes (at smaller pH values) manifest in the frequency shift of bands in the range of quinoid carbonyl ν(C3=O_q; 1645 cm^{-1}) and symmetric vibrations of the endocyclic ν(φ−N=C) groups (1274 cm^{-1}), and also in the redistribution of the intensity of antisymmetric vibrational bands of the endocyclic groups of the phenoxazone chromophore ν(C−C=C) and ν(φ−N=C) (1463 and 1500 cm^{-1}, respectively) and of amino group ν(C2−NH_2) (1396 and 1418 cm^{-1}). Observed changes in acid pH range resulting from either hydrolysis of phenoxazone ring or amino-imino equilibrium of chromophore[14] require more detailed studies.

Titration Curves and Raman Spectra of Diaminoactinocin

It is seen from Fig. 3a that the pH-titration curve of the diaminoactinocin (AAct) is biphasic. We assume that the H^+ binding to AAct occurs in two steps, and this is probably related to the existence of two $-\overset{\overset{O_R}{\|}}{C}-NH_2$ and $-\overset{\overset{O_L}{\|}}{C}-NH_2$ amide groups in the AAct molecule (Fig. 1b).

The concentration of bound protons per AAct mole at the end of titration was obtained as

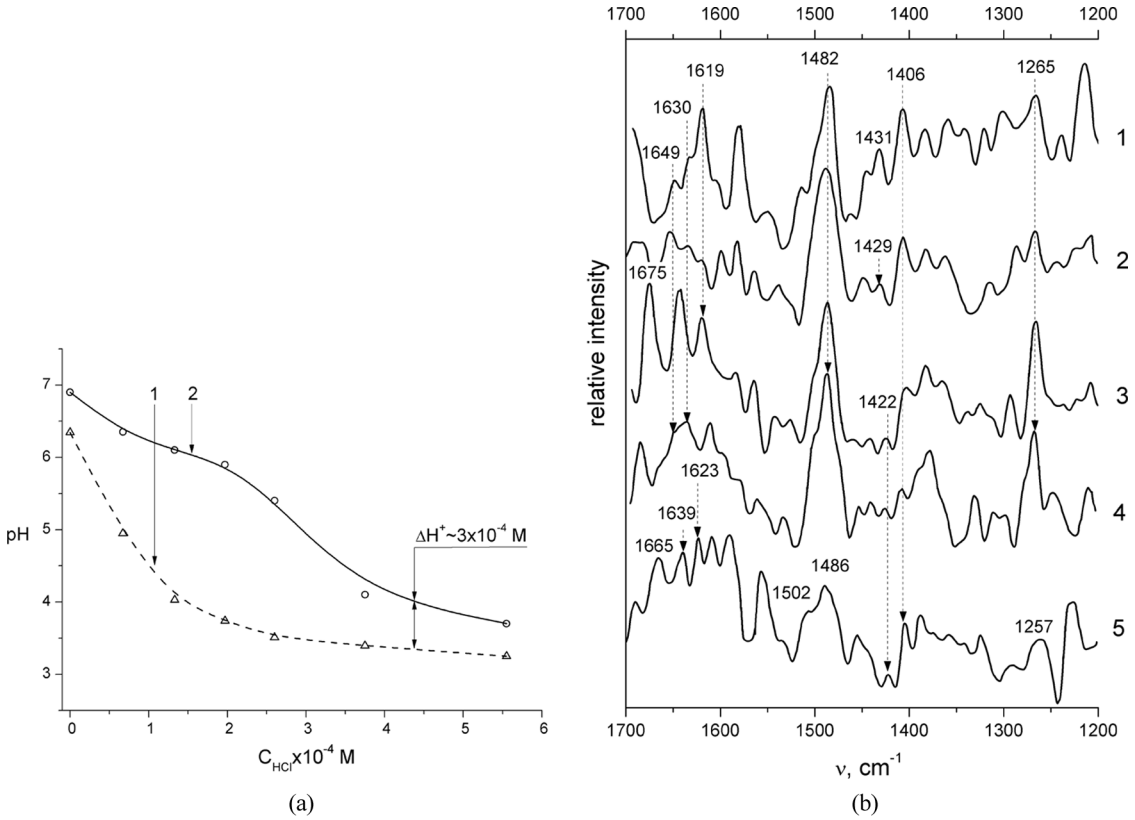

FIGURE 3 **(a) Experimental titration curves of (1) HCl solution (control) and (2) HCl solution in the presence of AAct. (b) Raman spectra of diaminoactinocin at pH (1) 6.86, (2) 5.25, (3) 4.15, (4) 3.75, and (5) 3.40. Concentration of AAct was constant $C_{AAct} = 1.5 \times 10^{-4}$ M. Error bars are smaller than the corresponding symbols at the titration curves.**

$\Delta H^{+}_{max} = 3 \times 10^{-4}$ M at the $C_{AAct} = 1.5 \times 10^{-4}$ M. Hence, in this pH range, there are two protonated groups. In order to describe the protonation in such a case, we used the following model:

$$D + H^{+} \overset{K_1}{\longleftrightarrow} DH^{+}, DH^{+} + H^{+} \overset{K_2}{\longleftrightarrow} DH_2^{2+}.$$

The equilibrium constants can be expressed as

$$K_1 = \frac{[DH^{+}]}{[D] \cdot [H^{+}]} \quad (1)$$

$$K_2 = \frac{[DH_2^{2+}]}{[DH^{+}] \cdot [H^{+}]} \quad (2)$$

In the above written equations, [H^+], [D], [DH^+], and [DH^{2+}] represent the equilibrium concentrations of protons and unprotonated and protonated ligands, respectively. These concentrations in each mixture (C_D, C_{HCl}) have been calculated using Eqs. (1)–(4), taking into account the ionic product for water that $[H^{+}] \cdot [OH^{-}] = 10^{-14}$:

$$C_D = [D] + [DH^{+}] + [DH_2^{2+}] \quad (3)$$

$$C_{Cl^-} = [DH^{+}] + 2[DH_2^{2+}] + [H^{+}] - [OH^{-}] \quad (4)$$

Equations (3) and (4) represent the laws of mass and charges conservation, respectively. The optimal K_1 and K_2 values for AAct were obtained by fitting the experimental titration curve to the calculated pH-dependence by Eqs. (1)–(4) as $\log K_1 = 6.9 \pm 0.5$ and $\log K_2 = 5.3 \pm 0.1$.

When comparing the Raman spectra of neutral solution of aminophenoxazone (Fig. 2b) and diaminoactinocin (Fig. 3b), it is possible to note that their difference is mainly observed in the range of vibrations of C=O groups and symmetric and asymmetric vibrations of endocyclic groups of a phenoxazone ring. It is likely that the appearance of two amide groups in AAct molecule influences vibrations of base functional groups of the phenoxazone chromophore. Please note that instead of a single strongly pronounced band at $\nu = 1645\ \mathrm{cm}^{-1}$ for Aph (Fig. 2b, pH 6.4), feebly marked bands at $\nu \sim 1630$ ($C3{=}O_q$) and $\sim 1649\ \mathrm{cm}^{-1}$ ($C{=}O_R$) for AAct are obtained. From Raman spectrum 3 (Fig. 3b), there is an appearance of a band at $1672\ \mathrm{cm}^{-1}$, which are attributed to the $C{=}O_L$ of the second amide group. This fact can testify that the second amide

group of the AAct molecule is titrated at pH $\leq$ 4.15. It is clearly seen from the Raman spectra (Fig. 3b, spectra 2–5) that the frequency shift of the C=O_L band depends on pH. The 1665 cm^{-1} band has been assigned to completely protonated AAct at pH ~3.5. At pH < 3.5, the Raman spectrum of AAct (Fig. 3b, spectra 5) shows the degradation of the sample, as described above for Aph. Thus, the existence of two amide groups in the 1 and 9 positions of chromophore do not influence on the stability of phenoxazone ring.

Titration Curve and Raman Spectra of Dimethylaminoalkyl Derivatives ActIII(1) and ActIII(2)

The titration curves of ActIII(1) and ActIII(2) ligands having different affinities to DNA are essentially different from each other and from Aph and AAct. As it can be seen from Fig. 4a, the apparent tendency for protonation of the ligand is observed on the ActIII(1) titration curve at relatively high pH values, while for the ActIII(2) ligand (Fig. 5a), the titration curve coincides with the control curve. The number of bound protons per mole of ActIII(1) is $\Delta H^{+}_{max}/C_{ActIII(1)} = 1$. It follows that the ActIII(1) molecule has only one binding site of H^{+} ions. Therefore, protonation of ActIII(1) can be described by Eqs. (1), (3), and (4). For this case, the optimal value of protonation constant is log $K = 5.3 \pm 0.1$.

Figure 4b shows the changes of Raman spectra of the ActIII(1) solution in the ranges of ν(C2−NH_2) vibration ($\nu \sim 1392$–$1426\,cm^{-1}$), endocyclic groups of a phenoxazone chromophore ν(C−C=C) and ν(φ−N=C) ($\nu \sim 1490\,cm^{-1}$), and carbonyl groups ($\nu \sim 1615$–$1661\,cm^{-1}$) at pH decreasing. In contrast to ActIII(1), Raman spectra of the ActIII(2) sample (Fig. 5b) do not display the essential changes of spectral parameters (shifts of Raman bands) in the considered pH range. Vibration bands of endocyclic

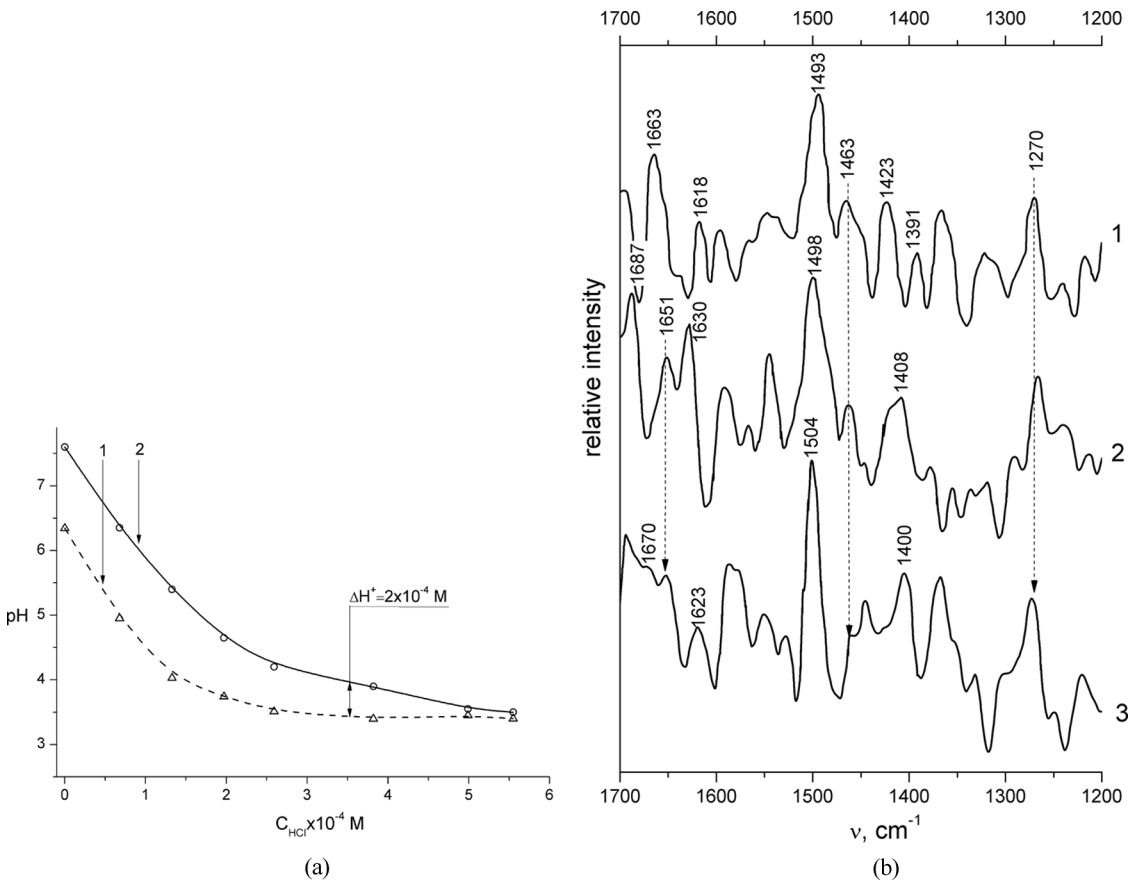

FIGURE 4 (a) Experimental titration curves of (1) HCl solution (control) and (2) HCl solution in the presence of ActIII(1). (b) Raman spectra of ActIII(1) at pH (1) 7.60, (2) 4.70, and (3) 3.70. Concentration of ActIII(1) was constant $C_{ActIII(1)} = 2 \times 10^{-4}$ M. Error bars are smaller than the corresponding symbols at the titration curves.

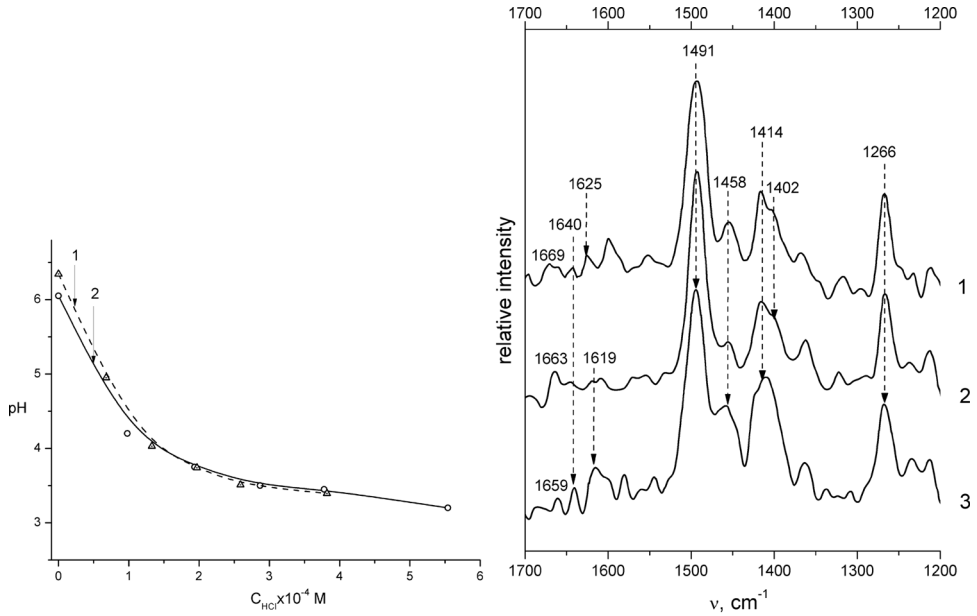

FIGURE 5 **(a) Experimental titration curves of (1) HCl solution (control) and (2) HCl solution in the presence of ActIII(2). (b) Raman spectra of ActIII(2) at pH (1) 6.10, (2) 4.20, and (3) 3.50. Concentration of ActIII(2) was constant $C_{ActIII(2)} = 2.1 \times 10^{-4}$ M. Error bars are smaller than the corresponding symbols at the titration curves.**

ν(C−C=C) and ν(φ−N=C) groups (1491 and 1266 cm^{-1}) are not changed, even at rather low pH values (Fig. 5b). In the region of carbonyl vibrations ($\nu = 1620$–1670 cm^{-1}), sufficiently clear-cut and reproducible spectra was not obtainable, therefore these results are not discussed here.

Comparing Figs. 4b and 5b, a significant difference is noted between the Raman spectra of the ActIII(1) and ActIII(2) samples in both neutral and acid solutions (spectra 1 and 3, respectively). This fact is explained by the different structures of these samples, as synthesis of actinocin derivatives is a multistage process. Therefore, it is difficult to separate the individual synthesized (nonsymmetrical and symmetrical) samples.[8]

Titration Curves of Dimethylaminoalkyl Derivatives ActII–ActV

Figure 6 represents the titration curves of actinocin derivatives with different numbers of methylene groups in the side chain (ActII–ActV). It is possible to note that the derivatives with four and five methylene groups (ActIV and ActV) are not practically protonated in the chosen range of HCl concentrations.

Binding of Actinocin Derivatives to Thymus DNA at Different Ionic Strengths

Figure 7 shows the absorption spectra of mixtures of the ActIII(1) and ActIII(2) cations with calf thymus DNA at the constant total concentration of ligands. It can be seen that the absorption spectra of

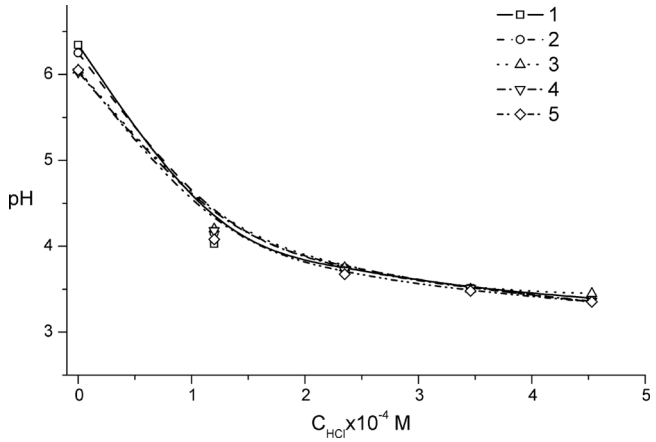

FIGURE 6 **Experimental titration curves of actinocin derivatives with dimethylaminoalkyl side chains having different number of methylene groups: (1) control; (2) ActII, $C_{ActII} = 3.3 \times 10^{-5}$ M; (3) ActIII(2), $C_{ActIII(2)} = 2.1 \times 10^{-4}$ M; (4) ActIV, $C_{ActIV} = 4.2 \times 10^{-5}$ M; and (5) ActV, $C_{ActV} = 7.8 \times 10^{-5}$ M. Error bars are smaller than the corresponding symbols at the titration curves.**

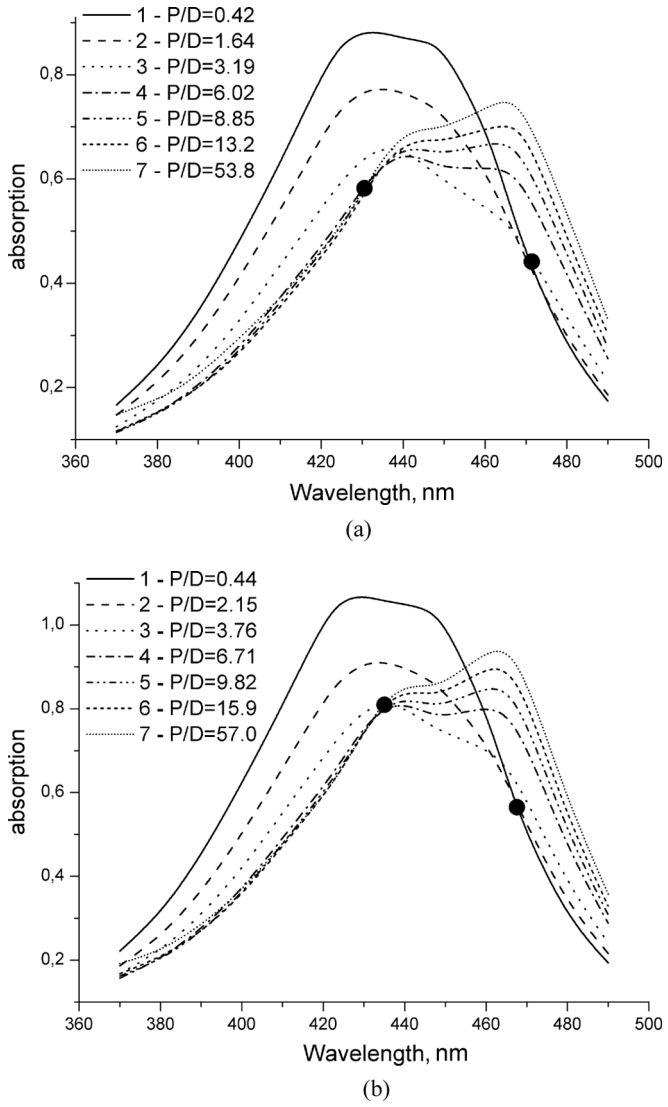

FIGURE 7 **Absorption spectra of ActIII(2)-DNA (a) and ActIII(1)-DNA (b) mixtures at constant concentration of ActIII(2) ($C_{ActIII(2)} = 3.16 \times 10^{-5}$ M) and ActIII(1) ($C_{ActIII(1)} = 4.07 \times 10^{-5}$ M) and different DNA concentrations in solution at 2×10^{-2} M NaCl, pH 6.86. The closed circles denote the isosbestic points.**

ActIII(2)-DNA and ActIII(1)-DNA mixtures at each constant ActIII concentration in broad DNA concentration range intersect at the two wavelengths; i.e., there are two isosbestic points. That is why it is assumed that in those Act-DNA systems, at least two types of complexes are formed. Similar conclusions were made in many experimental works for different ligand-DNA systems.[9,15–17] The first type of complexes is formed at low P/D values, the second type is formed at high values of P/D (where P is the concentration of polynucleotide, and D is the concentration of ligand).[8,10]

The binding constants of these ligands to DNA were calculated by the two type binding model in

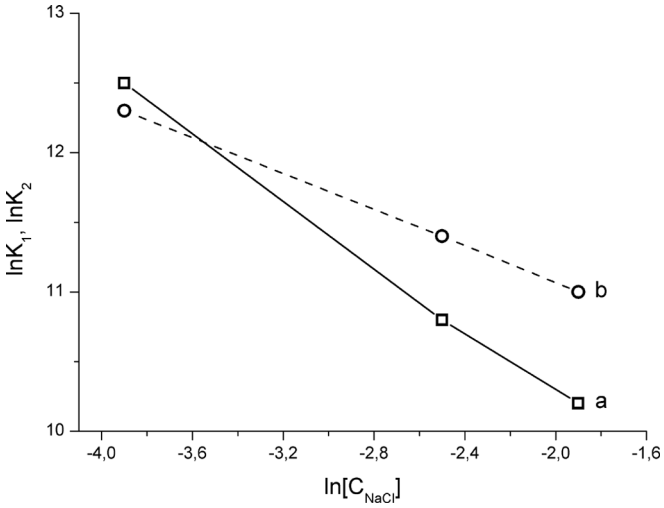

FIGURE 8 **Dependences of binding constants of ActIII(2) (a) and ActIII(1) (b) to calf thymus DNA for the complexes of outside type on ln [NaCl] concentration, pH 6.86.**

solutions with different NaCl concentrations using the DALSMOD program.[18,19] Figure 8 shows the logarithmic dependencies of the obtained binding constants on NaCl concentration for the intercalation of the first type of ActIII(2)-DNA and ActIII(1)-DNA complexes. It can be seen that values of these constants do not practically differ for ActIII(2) and ActIII(1) ligands in solutions with low NaCl concentration. Nevertheless, the plots of these dependencies on ln [NaCl] (α) indicate essential differences. The slopes of the logarithmic plots in Fig. 8 are $\alpha_1 = -1.15$ for ActIII(2) and $\alpha_1 = -0.65$ for ActIII(1). According to the polyelectrolyte theory of Record et al.,[20] Sharp,[21] and Misra and Honig,[22] the distinction between α values is more consistent with the lesser value of the ActIII(1) molecule charge in solution at pH 6.86 than for ActIII(2). This conclusion is in good agreement with our titration results for these drugs presented above.

Similarly, we suppose that the observed differences of the biological activities of ActIII(2) and ActIII(1) ligands can be explained not only by various length and structures of their side chains[1,2] but, to some extent, by differences in values of positive charges of these molecules in neutral solutions. This can lead to various molecular mechanisms of complex formation of these ligands to DNA matrix.

CONCLUSIONS

The actinocin derivatives with a different structure of side chains have been investigated by the methods

of spectrophotometry, pH-metry, and Raman spectroscopy. It has been shown that the investigated samples of actinocin derivatives have a different charge of cation in neutral water solutions. For the first time, the assignment to characteristic frequencies of Raman spectra of the main functional groups of actinocin derivatives in protonated and nonprotonated states has been made. Comparison of Raman spectra of newly synthesized actinocin derivatives has shown that the chemical modification of the phenoxazone ring starts only at low values of $pH < 3.5$. The actinocin derivatives ActII, ActIII(2), ActIV, and ActV are doubly charged cations in neutral solution. The analysis of interaction of ActIII(1) and ActIII(2) with DNA at various ionic strengths allowed the conclusion that these samples have different values of positive charge.

REFERENCES

1. Ovchinnikov, D. V.; Baranovsky, S. F.; Rozvadovska, A. O.; Rogova, O. V.; Veselkov, K. A.; Ermolaev, D. V.; Parkes, H.; Davies, D. B.; Evstigneev, M. P. Structural basis for the binding affinity of a homologous series of synthetic phenoxazone drugs with DNA: NMR and molecular mechanics analysis. *J. Biomol. Struc. Dyn.* **2007**, *24*(5), 443–453.
2. Veselkov, A. N.; Maleev, V. Ya.; Glibin, E. N.; Karawajew, L.; Davies, D. B. Structure–activity relation for synthetic phenoxazone drugs. Evidence for a direct correlation between DNA binding and pro-apoptotic activity. *Eur. J. Biochem.* **2003**, *270*, 4200–4207.
3. Williams, M. C.; Wenner, J. R.; Rousina, I.; Bloomfield, V. A. Effect of pH on the overstretching transition of double-stranded DNA: Evidence of force-induced DNA melting. *Biophys. J.* **2001**, *80*, 874–881.
4. Moody, E. M.; Lecomte, J. T. J.; Bevilaqua, P. C. Linkage between proton binding and folding in RNA: A thermodynamic framework and its experimental application for shifting a K investigating. *RNA* **2006**, *11*(2), 157–172.
5. Gale, E. F.; Cundliffe, E.; Reynolds, P. E.; Richmond, M. H.; Waring, M. J. *The Molecular Basis of Antibiotic Action*; Wiley-Interscience Public: London, 1972; 337.
6. Barbieri, M.; Pilch, D. S. Complete thermodynamic characterization of the multiple protonation equilibria of the aminoglycoside antibiotic paromomycin: A calorimetric and natural abundance ^{15}N NMR study. *Biophys. J.* **2006**, *90*, 1338–1349.
7. Antipov, A. A.; Sukhorukow, G. B. Polyelectrolyte multilayer capsules as vehicles with tunable permeability. *Adv. Col. Interfer. Sci.* **2004**, *11*, 49–61.
8. Veselkov, A. N.; Davies, D. B., Eds. *Anti-Cancer Drug Design: Biological and Biophysical Aspects of Synthetic Phenoxazone Derivatives*; SevNTU Press: Sevastopol, 2002.
9. Maleev, V.; Semenov, M.; Kruglova, E.; Bolbukh, T.; Gasan, A.; Bereznyak, E.; Shestopalova, A. Spectroscopic and calorimetric study of DNA interaction with a new series of actinocin derivatives. *J. Mol. Struc.* **2003**, *645*, 145–158.
10. Kruglova, E. B.; Gladkovskaya, N. A.; Maleev, V. Ya. Use of spectrophotometric analysis to calculate the thermodynamic parameters of binding between an actinocin derivative and DNA. *Biophysics (Rus.)* **2005**, *50*(2), 243–254.
11. Moore, S.; Kondo, M.; Copeland, M.; Meienhofer, J. Synthesis and antitumor activity of 2-Deamino- and W- (7-Hydroxypropy1)actinomycin D1. *J. Med.Chem.* **1975**, *18*(11), 1098–1101.
12. Yoo, H.; Rill, R. L. Single-strand DNA binding of actinomycin D with a chromophore 2-amino to hydroxyl substitution. *J. Biocem. Mol. Biol.* **2003**, *36*(3), 305–311.
13. Smulevich, G.; Angeloni, L.; Marzocchi, M. Raman excitation profiles of actinomycin D. *Biochim. Biophys. Acta* **1980**, *610*, 384–391.
14. Chinsky, L.; Turpin, P. Y. Fluorescence of actinomycin D and its DNA complex. *Biochim. Biophys. Acta* **1977**, *475*, 54–63.
15. Sovenyhazy, K. M.; Bordelon, J. A.; Petty, J. T. Spectroscopic studies of the multiple binding modes of a trimethine-bridges cyanine dye with DNA. *Nucleic Acids Res.* **2003**, *31*, 2561–2569.
16. Biver, T.; DeBiasi, A.; Fernando Secco, F.; Venturini, M.; Yarmoluk, S. Cyanine dyes as intercalating agents: Kinetic and thermodynamic studies on the DNA/Cyan40 and DNA/CCyan2 systems. *Biophys. J.* **2005**, *89*, 374–383.
17. de Abreu, F. C.; de Paula, F. S.; Ferreira, D. C. M.; Nascimento, V. B.; Santos, A. M. C.; Santoro, M. M.; Salas, C. E.; Lopes, J. C. D.; Coulart, M. O. F. The application of DNA-biosensors and differential scanning calorimetry to the study of the DNA-binding agent berenil. *Sensors* **2008**, *8*, 1519–1538.
18. Kruglova, H. B. A possible approach to account the counterion effect on the complex formation in polyelectrolyte-ligand system. *J. Mol. Biol. (Rus.)* **1991**, *25*, 60–68.
19. Kruglova, H. B.; Zinenko, T. L. Experimental and theoretical studies of DNA complex formation with coloured biologically active ligands depending on the ionic strength of solution. *Mol. Biol. (Rus.)* **1993**, *27*(3), 655–665.
20. Record, M. T.; Anderson, C. F.; Lohman, T. M. Thermodynamic analysis of ion effects on the binding and conformational equilibria of proteins and nucleic acids: The roles of ion association or release, screening, and ion effects on water activity. *Quart. Rev. Biophys.* **1978**, *11*, 102–178.
21. Sharp, K. A. Polyelectrolyte electrostatics: Salt dependence, entropic and enthalpic contributions to free energy in the nonlinear Poisson-Boltzmann model. *Biopolymers* **1995**, *36*, 227–243.
22. Misra, V. K.; Honig, B. Proceedings on the magnitude of the electrostatic contribution to ligand-DNA interactions. *Natl. Acad. Sci. USA* **1999**, *92*(10), 4691–4695.